Composites Science and Technology 76 (2013) 29–36

Contents lists available at SciVerse ScienceDirect

Composites Science and Technology

journal homepage: www.elsevier.com/locate/compscitech

Dielectric constant and breakdown strength of polymer composites with high aspect ratio fillers studied by finite element models

Zepu Wang [a,*], J. Keith Nelson [b], Henrik Hillborg [c], Su Zhao [c], Linda S. Schadler [a]

[a] Department of Material Science and Engineering, Rensselaer Polytechnic Institute, Troy, NY 12180, USA
[b] Department of Electrical, Computer and Systems Engineering, Rensselaer Polytechnic Institute, Troy, NY 12180, USA
[c] ABB AB, Corporate Research, Power Technology, Västerås SE-721 78, Sweden

ARTICLE INFO

Article history:
Received 26 September 2012
Received in revised form 16 December 2012
Accepted 20 December 2012
Available online 5 January 2013

Keywords:
A. Polymer–matrix composites (PMCs)
B. Electrical properties
C. Finite element analysis (FEA)
C. Modelling

ABSTRACT

A finite element model was used to study the dielectric constant and breakdown strength of polymer composite filled with high aspect ratio fillers. The impact of composite microstructure and filler aspect ratio on the dielectric properties was investigated. The results were used to explain the experimental data for $BaTiO_3$ fiber filled poly(dimethyl siloxane) published previously. The effect of filler shape, aspect ratio distribution, curvature, grain boundary and alignment on the composite permittivity was studied. A model was proposed to correlate the composite microstructure, the electric field distribution in the polymer matrix, and the dielectric breakdown strength of composites.

1. Introduction

Ferroelectric ceramic particles with high dielectric constant are widely used to increase the dielectric constant of polymer composites for energy storage applications. However, according to the rule of mixtures, the increase in composite permittivity is small for spherical fillers especially at low volume fractions. The permittivity of composites with high aspect ratio (AR) fillers increases more rapidly with loading [1]. Recently, traditional inorganic materials have become available in high AR forms [2–6]. Some of those new materials have a high dielectric constant, and can be processed with controlled geometry.

Analytical models based on effective medium theory (such as the rule of mixtures) can be used to predict composite permittivity [1]. The analytical models are accurate when the filler volume fraction is low, but do not consider filler–filler interaction and filler dispersion. Numerical approaches such as finite element analysis and finite difference methods can be used to predict the electric field and permittivity based on the properties of individual phases and the detailed composite microstructure. Some early work using 2-dimensional periodic models found reasonable agreement for the effective permittivity between the two approaches [7–9]. 3-dimensional finite element (FE) and finite difference (FD) simulations have been used to predict the effective permittivity of composites, and the results were compared to experimental data [10–13]. The numerical simulations fit the experimental data better because they include particle geometry, dispersion and distribution. Only a few numerical modeling studies have focused on high AR fillers [14,15] and simple geometries with a few fillers were used due to computing limitations.

In our previous work [16], polymer composites filled with electrospun $BaTiO_3$ fibers showed that the dielectric constant and breakdown strength depended on filler AR. The results are summarized in Table 1. The composite permittivity was below the Maxwell Garnett (MG) rule of mixtures prediction [17] for high AR fillers, while the composites with low AR fillers matched the prediction. The MG equation is supposed to be accurate at the low filler volume fraction, 0.2, used in the study. However, there are several differences between the model and the real composite as listed below.

- Ellipsoidal fillers are considered in the rule of mixtures and the real fibers have a rod-like or capsule-like shape.
- The distribution in fiber AR may affect the dielectric constant.
- There were grain boundaries in the $BaTiO_3$ fibers. These low dielectric constant grain boundaries separate the high dielectric constant fiber into many lower AR segments, which might lead to a reduction in the composite permittivity.
- Real fibers have curvature which is not considered in the rule of mixtures. High AR fillers have a larger tendency to bend in the composite.

* Corresponding author.
E-mail address: zepu.wang@ieee.org (Z. Wang).

0266-3538/$ - see front matter © 2013 Elsevier Ltd. All rights reserved.
http://dx.doi.org/10.1016/j.compscitech.2012.12.014

Table 1
Summary of the permittivity and breakdown strength of $BaTiO_3$ fiber filled composite in [16].

Aspect ratio (AR)	Neat polymer	3	3	6	6	15	15
Filler volume fraction		0.1	0.2	0.1	0.2	0.1	0.2
Permittivity	3.02	4.53	6.38	4.90	8.33	7.47	11.97
BD strength[a] (kV/mm)	31.5	–	–	23.2	19.1	18.3	15.3

[a] BD strength represents the 63% probability value in the Weibull distribution of dielectric breakdown strength.

- Fiber alignment cannot be completely avoided in the compression molding process. Filler alignment in the sample plane decreases the out-of-plane dielectric constant.

The five reasons stated above are potential explanations for the difference between the MG model prediction and the experimental results. However, the impact of each proposed mechanism is difficult to differentiate using experiments. In this work, finite element analysis (FEA) was performed in both 2D and 3D models to examine the influence of each factor on the dielectric constant. The goal is to evaluate the applicability of the MG rule of mixtures for composites with high AR fillers, and the impact of composite microstructure on the effective permittivity.

In addition, finite element simulations can provide a statistical view of the local electric field distribution in the polymer. When high dielectric constant fillers are used, the polymer matrix sustains most of the electric stress. The local enhanced field can be linked to the electrical breakdown strength for a short term breakdown process. A statistical analysis of the local field in the polymer was performed to obtain a comprehensive understanding of the field enhancement by high permittivity fillers and its effect on the composite breakdown strength.

2. Finite element analysis (FEA) approach

The methodology for 3D simulations is presented. The 2D models followed a similar approach. The FEA was performed using commercial software, COMSOL Multiphysics and MATLAB. High AR fillers were represented by elongated capsules consisting of a cylinder with two semi-spheres at the ends (Fig. 1a). The AR was calculated as the ratio of the end-to-end length and the diameter of the cylinder. An AR of one reduces the geometry to a spherical particle. To compare filler shapes, ellipsoidal fillers were also studied because ellipsoids are considered in the rule of mixtures.

The composites were represented as cubes (Fig. 1d). To ensure random filler orientation, the orientation parameters were pregenerated for each filler, following a uniform distribution from a pseudorandom number generator. The fillers were then added into the cube using Random Sequential Addition (RSA) to avoid overlapping of fillers. While the position parameters followed a uniform distribution in the box, two parameters in spherical coordinates, φ and θ, were used as the orientation parameters as shown in Fig. 1c. To ensure a uniform distribution of filler orientation, the following equations were used, where φ and t followed a uniform distribution over the designated range.

$$\varphi = [0, 2\pi] \tag{1}$$

$$\theta = arccos(t) \tag{2}$$

$$t = [-1, 1] \tag{3}$$

To ensure a continuous electrical field and avoid edge effects, a 3D periodic geometry was used to form an infinite composite material. In addition, periodic electric boundary conditions were applied to the six faces of the cube. For the boundaries of the cube in the x and y directions, the potential of any two corresponding points on the opposite boundary were set to be the same, so the tangential electric field was continuous across the periodic boundary. For the two boundary faces in the z direction where an electrical potential drop was applied, a constant voltage difference was set to each of the corresponding points with the same x and y coordinates. In this way, the potential drop along the z axis is continuous and constant across every repeating unit, which is essentially equivalent to the situation of an infinite size material immersed in an applied electric field. A 2D model filled with high permittivity particles is shown in Fig. 1b for simplicity of illustration.

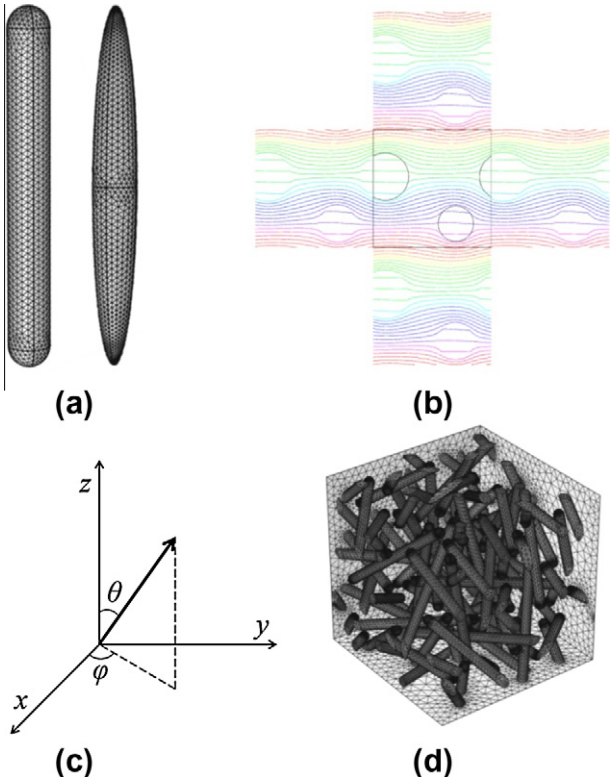

Fig. 1. Illustration of model; (a) the elongated capsular and ellipsoidal filler; (b) 2D periodic box with particles showing the repeating geometry and continuous electrical field at boundaries; field is applied in the vertical direction; equipotential lines are plotted; the center box is the actual model; (c) the spherical coordinates used to define the orientation of fillers; and (d) a 3D model with 50 fillers.

This work focuses on high dielectric constant fillers. The material properties used are listed in Table 2. The field distribution and effective dielectric constant of composites is not sensitive to filler permittivity once the permittivity contrast between filler and polymer is large enough. For example, when the filler dielectric constant varies from 500 to 5000, the composite dielectric constant (according to the rule of mixtures) increases from 5.28 to 5.47 in a composite with a filler AR of 5 and a filler volume fraction of 0.1. For this reason, the permittivity of filler was set to 1000 to represent the $BaTiO_3$ fiber even though the exact permittivity of the prepared $BaTiO_3$ fibers is unknown and different permittivity values from 500 to 10,000 have been reported in the literature [18,19]. Moderate anisotropy was observed with less than 50%

Table 2
Material properties used in the FEA.

	Permittivity	Loss factor
Filler	1000	0.01
Polymer	3	0.001

variation in the dielectric constant along different crystal orientations [20,21]. Because the composite dielectric constant is not sensitive to this magnitude of variation for the high dielectric constant fillers, an isotropic dielectric constant was assigned to the $BaTiO_3$ fibers for the simplicity of simulation. A loss factor of 0.01 was assigned to the filler [22]. Because the imaginary permittivity is 1/100 of the real permittivity, the latter is the dominant factor causing the increase in the composite permittivity.

The study was carried out in the frequency domain of the harmonic field condition. The frequency of the applied ac field was set to 100 Hz. The effective permittivity of the composites was calculated from the constitutive relation of the electric flux density D and the electric field E [1], which is shown in Eq. (4). $\langle f \rangle$ represents the spatial average of a physical quantity over a certain volume.

$$\langle D \rangle = \varepsilon_{eff} \langle E \rangle \tag{4}$$

The composite permittivity was evaluated as a function of the number of fillers. It was found that 100 fillers lead to a representative geometry while maintaining computational simplicity. The electric field in the polymer matrix was sampled and plotted as a probability distribution function of the local field relative to the applied field.

3. Result and discussion

3.1. Dielectric constant

3.1.1. FEA results compared with MG rule of mixtures – effect of filler shape

The applicability of the rule of mixtures to composites with high AR fillers was examined. Fig. 2 shows a comparison between the FEA results and the MG rule of mixtures. Since the rule of mixtures uses ellipsoidal fillers in the derivation and $BaTiO_3$ fibers have a capsular shape, a comparison of filler shape was performed to confirm whether the difference between experimental data and the rule of mixtures was from the particular shape of the $BaTiO_3$ fibers. The FEA results agree with the MG prediction at low filler loading, and are slightly higher for the filler volume fraction above 0.1. The filler shape does not affect the composite permittivity significantly given the same filler AR.

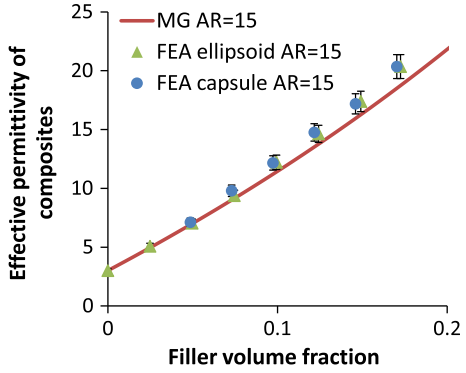

Fig. 2. A comparison between the FEA results and the Maxwell Garnett rule of mixtures; both results for elongated capsule shaped fillers and ellipsoidal fillers are plotted; error bars are one standard deviation derived from 10 simulations.

3.1.2. Effect of filler aspect ratio distribution

The MG rule of mixtures assumes the fillers have uniform AR. Although a precise control of filler AR is desired in the processing of composites, a distribution of filler AR exists and the effect on the composite dielectric constant is unknown. To investigate the effect of filler AR distribution, the AR of fillers was generated following a normal distribution in a 3D model. In this study, the average filler AR was set to 15 and a filler volume fraction of 0.1 was used. The relative standard deviation of the normal distribution was varied from 0 to 1. Any negative filler AR generated was excluded and any filler AR larger than twice the average was also excluded to keep the distribution symmetric. The results are shown in Fig. 3. A larger distribution of fiber AR increases the composite permittivity at a given constant average AR. However, the increase in the composite permittivity cannot explain the lower permittivity observed in the experiments.

3.1.3. Effect of grain boundary in the ferroelectric fillers

$BaTiO_3$ grain/particle consists of a tetragonal core with high permittivity and a cubic surface layer with low permittivity [23,24], resulting in low dielectric constant regions at the surface and grain boundaries of $BaTiO_3$ as illustrated in Fig. 4a. The cubic phase at the $BaTiO_3$ surface does not have a strong influence on the composite permittivity because the calculated volume fraction is 0.0014 of the filler volume, based on the reported cubic layer thickness of 15 nm [25] and a fiber diameter of around 800 nm. On the other hand, the cubic phase at the grain boundary could change the composite permittivity since it separates the fiber into several sections with lower AR as shown in Fig. 4b and c.

The effect of grain boundaries in the $BaTiO_3$ fibers was studied by 2D FEA to evaluate the field distribution around fillers. Fig. 5a and b shows the geometric arrangement of several fibers without or with grain boundaries placed in an external electric field of 1 kV/mm. The fiber length was 12 μm and the diameter was 0.8 μm according to experiment [16]. The size of the low permittivity region around the grain boundary of $BaTiO_3$ was set to 100 nm and the dielectric constant of that region ranged from 10 to 500 according to the literature [19,23,25–30]. Fig. 5c and d shows the height plot of the electric field strength with and without the existence of grain boundaries. The area near the tip of the fiber is under higher, while the polymer along the fiber sustains reduced stress. The field distribution was very similar for the two conditions upon a close check of the field amplitude at around the fillers. Varying the grain boundary permittivity from 10 to 500 caused no difference in the field distribution. The "aligned low AR segments" are equivalent to high AR fillers in terms of field distribution. Because a change in the composite effective permittivity fundamentally comes from a change in the field distribution within the polymer,

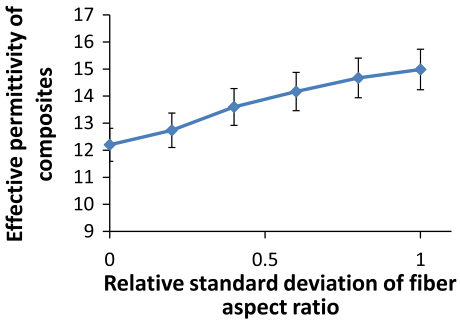

Fig. 3. A plot of the effective permittivity of composites with respect to the relative standard deviation of filler aspect ratio; average filler aspect ratio was 15 and filler volume fraction was 0.1; the error bar shows one standard deviation derived from 10 simulations.

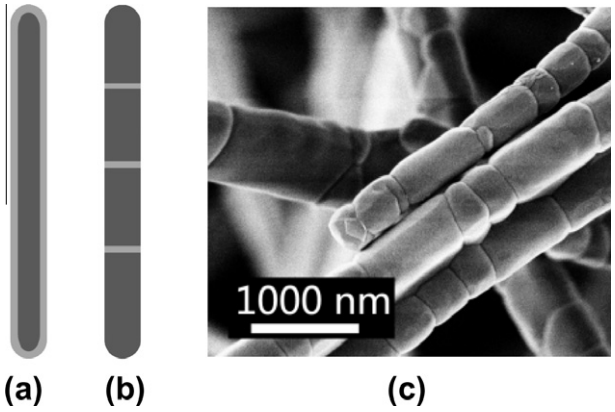

Fig. 4. Schematics of $BaTiO_3$ fibers, (a) with a cubic phase region at fiber surface; (b) with a cubic phase at the grain boundary; and (c) SEM image of $BaTiO_3$ fibers.

the composite permittivity is not affected by the low permittivity grain boundaries.

3.1.4. Filler curvature

$BaTiO_3$ fibers are curved in the composites. An optical microscopy image of the $BaTiO_3$ fiber composite is shown in Fig. 6a. Fibers with both large and small curvature can be identified. A simple 2D FEA was conducted to analyze the effect of filler curvature on the permittivity of composites. Several capsule-shaped fillers with an AR of 15 were dispersed in the polymer with the composite structure shown in Fig. 6c. The filler volume fraction was 0.1. To study the effect of filler curvature, the fillers were bent into arcs and the filler curvature is defined as the reciprocal of the arc radius. The arc length and width remained unchanged, as well as the position and orientation of the fillers.

The simulation result is shown in Fig. 6b. There is no change in the composite permittivity as the filler curvature increases. Although the result is based on a simple 2D simulation, the conclusion should be applicable to real composites. A qualitative explanation is provided as the following without a rigorous derivation. In the rule of mixtures, the effect of the high AR fillers is based on the reduction of the depolarization factor in the "high AR direction" [1]. The existence of the filler curvature increases the depolarization factor in the filler direction (average vector direction along the curved filler), but reduces the depolarization factor in the orthogonal direction. The average contribution of these two effects to the composites might be independent of filler curvature if the fillers are randomly orientated in the composites. As a result, the effective permittivity is independent of filler curvature for the composites with randomly orientated fillers. The curvature of the $BaTiO_3$ fibers, as shown in Fig. 6a, is smaller than the largest

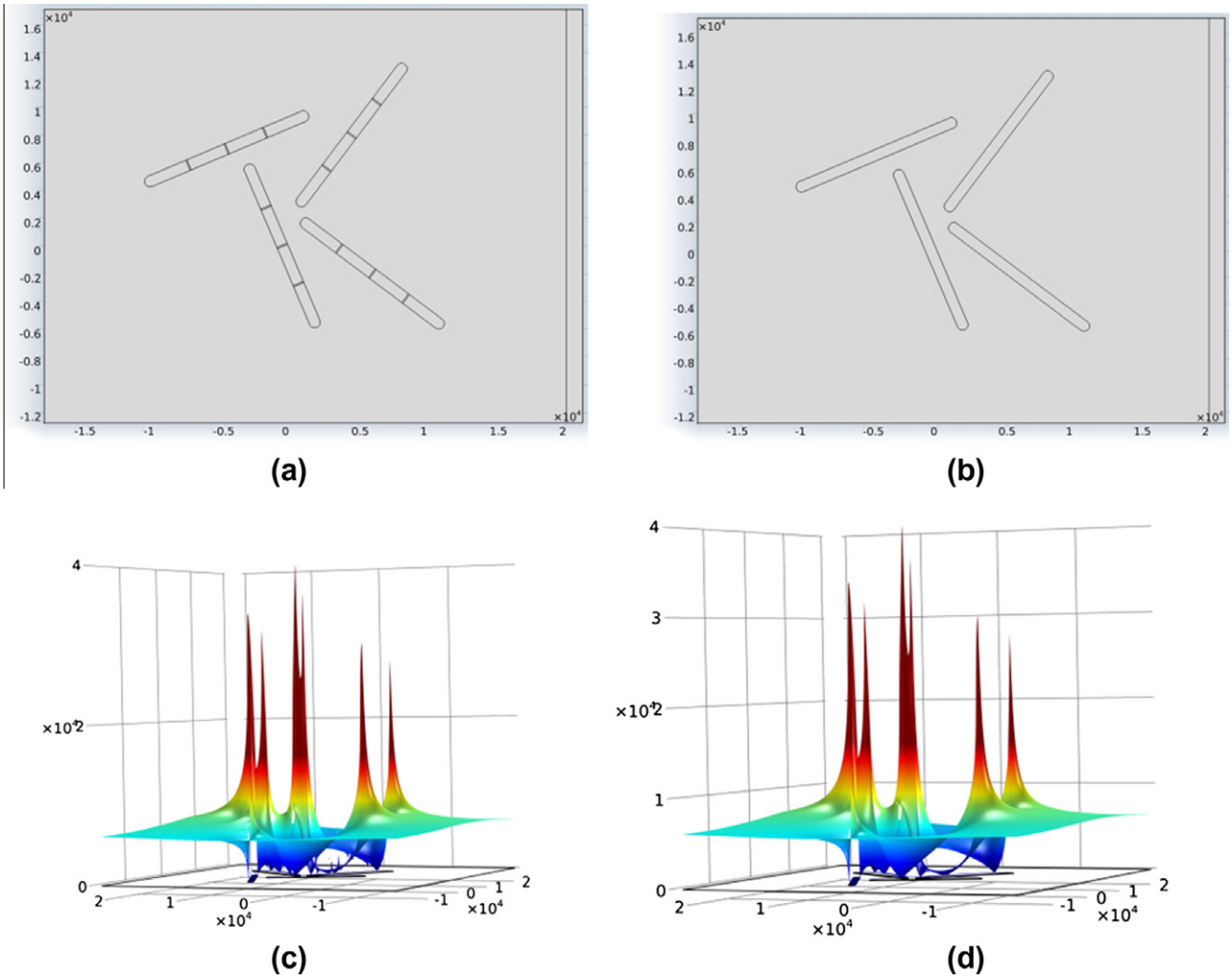

Fig. 5. (a and b) FEA geometry of composites, without or with grain boundaries respectively; (c and d) height plot of the electric field strength in the composites, without or with grain boundaries respectively.

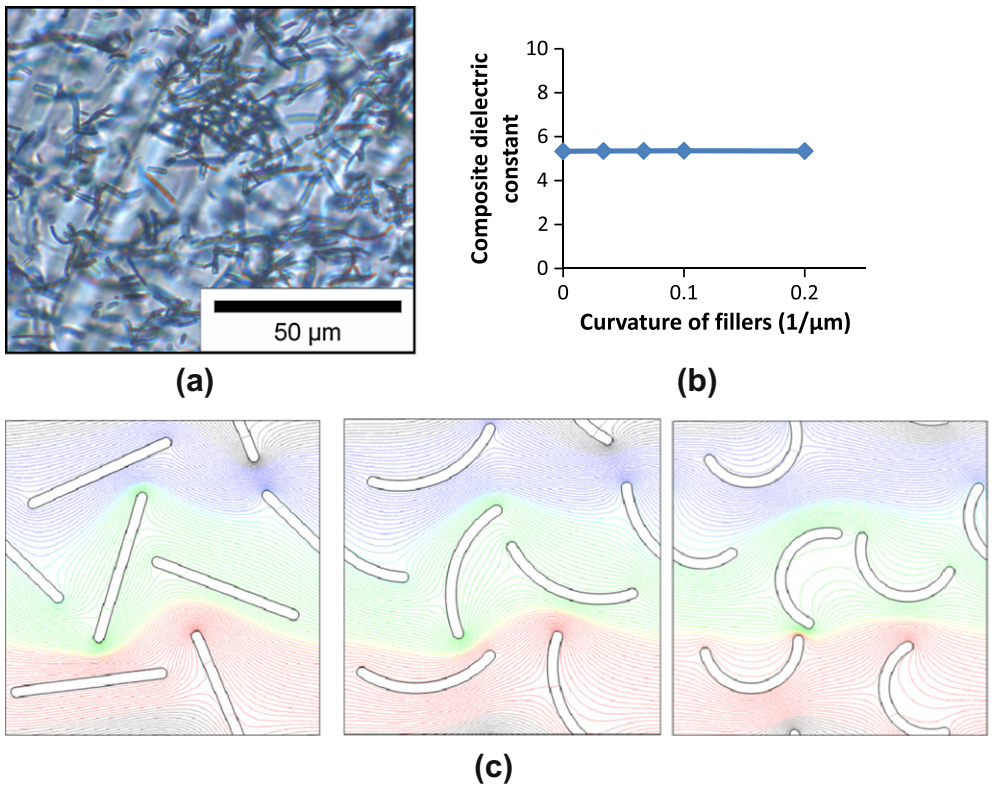

Fig. 6. (a) An optical microscopy image of $BaTiO_3$ fibers dispersed in PDMS; (b) the effect of filler curvature on the composite dielectric constant from 2D FEA; and (c) 2D FEA model with filler curvature of 0 (left), 0.1 (middle) and 0.2 (right) μm^{-1}.

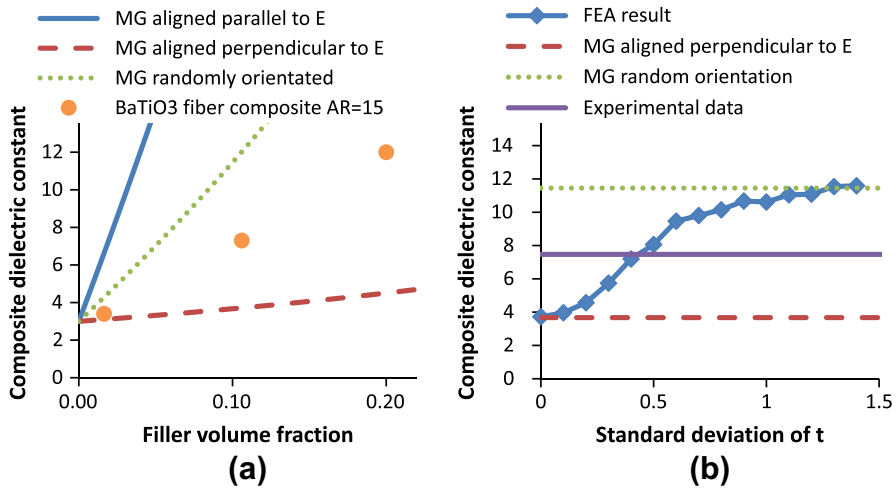

Fig. 7. (a) A comparison between the Maxwell Garnett rule of mixtures prediction with different alignment conditions and the experimental data with an aspect ratio of 15; and (b) the effect of filler alignment on the composite dielectric constant; a larger standard deviation of t corresponds to a more random orientation.

curvature used in the FEA. Thus the difference between the rule of mixtures prediction and the dielectric constant data does not come from filler curvature.

3.1.5. Filler alignment

Filler alignment creates an anisotropic dielectric constant. Alignment along the field direction increases the measured composite permittivity, while alignment perpendicular to the field direction reduces the permittivity. A comparison between the MG rule of mixtures and the experimental data is shown in Fig. 7a. The experimental data lies between the composites with randomly oriented fillers and fillers perfectly aligned perpendicular to the field direction. The comparison suggests that the fibers have a certain degree of alignment in the composites, if only the influence of filler alignment is considered.

To study the effect of fiber alignment in the compression molding process on the composite dielectric constant, the fiber orientation was set to follow a distribution function. The applied electric field is along the z-axis and the fibers are aligned in the xy-plane in the FEA. The orientation parameter t was randomly generated following a normal distribution with a mean value of 0 and a standard deviation ranging from 0 to infinity. Any value of t that was

out of the range, [−1, 1], was discarded. A standard deviation of 0 corresponds to perfect alignment in the *xy*-plane, while a standard deviation of infinity corresponds to completely random orientation. The composite dielectric constant is plotted as a function of the standard deviation of t ranging from 0 to 1.4 as shown in Fig. 7b. Increasing the standard deviation of t leads to a gradual transition in the composite permittivity from the aligned condition to the randomly orientated condition. A further increase in the standard deviation does not result in any significant increase in the composite dielectric constant. As shown in Fig. 7b, a standard deviation of 0.45 matches the experimental data. This partial alignment in the sample plane is likely from the compression molding process used to make the composites.

3.2. Breakdown strength

3.2.1. Modeling of electric field statistics in composites

The probability distribution function of the local electric field in the polymer normalized with respect to the applied electric field is plotted in Fig. 8a and b. The normalized electric field (*x*-axis in Fig. 8) can also be called the field intensification factor. The peak probability appears generally at a field that is slightly larger than the nominal applied electric field. The results suggest that a large portion (larger than 50%) of the polymer sustains intensified electric fields. The effect of filler AR is shown in Fig. 8a. Higher filler AR results in a larger tail in the high field side of the distribution plot. The probability of finding a local field that is larger than 3 times the applied field, calculated by integrating the probability distribution function, is plotted in Fig. 8c. The probability increases from 0.003 to 0.055 when the filler AR increases from 1 to 15. Consequently, the breakdown strength of the composite decreases because the breakdown is likely to initiate at those highly stressed spots. Similarly, the effect of filler AR is shown in Fig. 8b and d. The increase in filler volume fraction also broadens the probability distribution on the high electric field side and results in a reduction in the breakdown strength.

3.2.2. Quantitative comparison of modeling results and experimental data

A semi-empirical approach is presented to correlate the field distribution results from modeling and the experimental data of breakdown strength (E_B) shown in Fig. 3. To achieve this, it is necessary to define a characteristic value for the distribution of electric field obtained from the modeling. The average electric field strength or the average field strength modified by a fluctuation term has been used as the characteristic value, assuming they are inversely proportional to the breakdown strength [10,12]. In this work the field distribution is represented by a critical intensification factor (I_C), corresponding to a threshold field strength, than which 30% of the total polymer is under a higher stress as shown in Fig. 9a. I_C is designated as the characteristic value of the field intensification effect caused by the high permittivity fillers, and is considered to be inversely proportional to the electrical breakdown strength, E_B, as shown in Eq. (5), where the threshold value E_T is the short term breakdown strength of neat polymer measured at the same condition. This makes no assumptions about the mechanism of breakdown other than that it is facilitated by increased electric field.

$$I_c \times E_B = E_T \tag{5}$$

This argument is based on the assumption that once a certain portion (30% in this work determined empirically to fit the breakdown data) of polymer is under an electrical stress larger than the threshold value, electrical breakdown is observed. When the applied field on the composites is lower than the breakdown strength, less than 30% of polymer is under a field beyond the

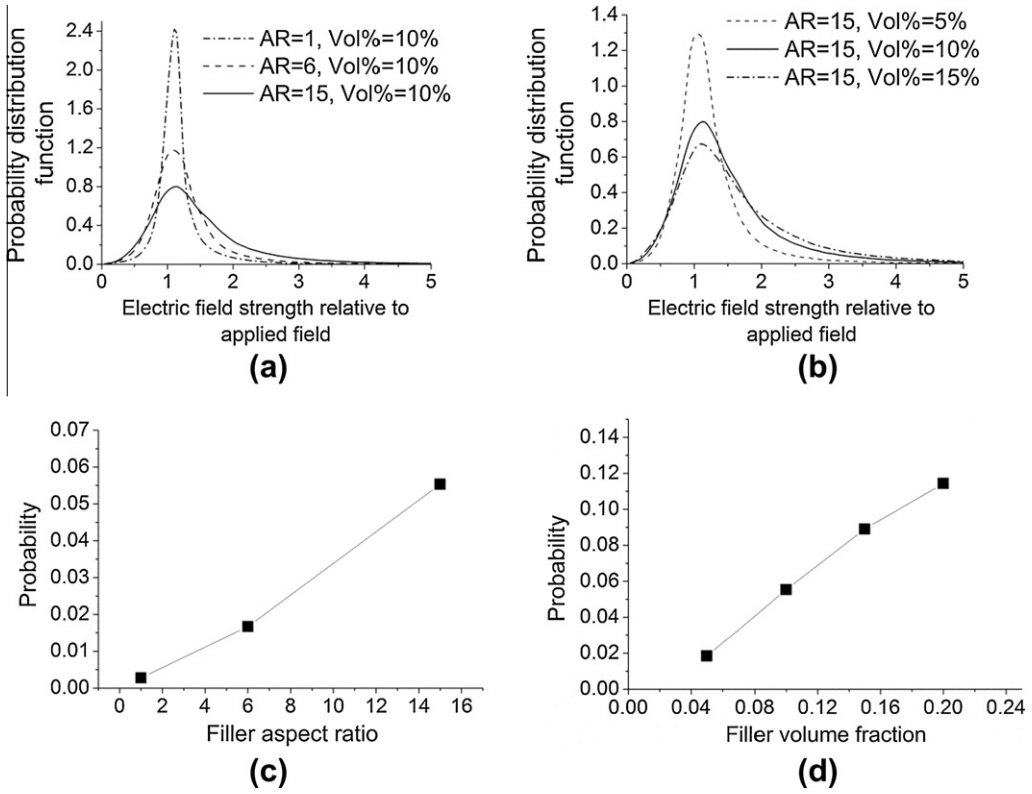

Fig. 8. Probability distribution function of the normalized electric field strength (relative to applied field) showing the effect of (a) filler aspect ratio and (b) filler loading; the probability of finding a local electric field that is larger than 3 times of the applied field showing the effect of (c) filler aspect ratio and (d) filler loading.

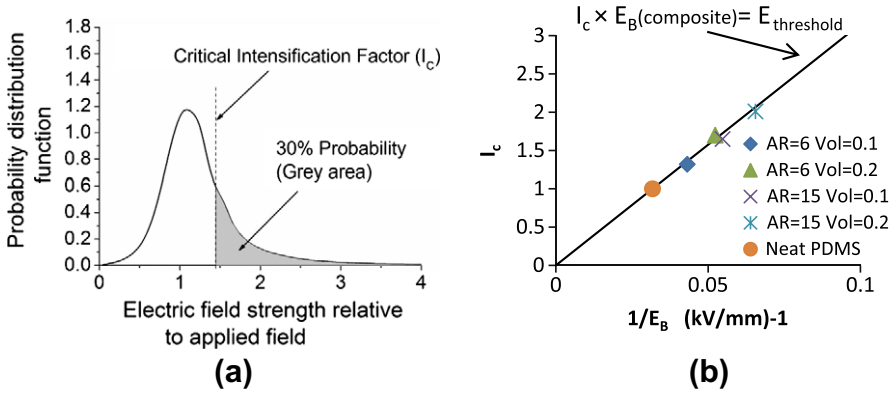

Fig. 9. (a) An illustration showing the definition of the critical intensification factor in this work, which is the boundary of the upper 30% of the field strength in polymer from FEA; and (b) the relationship between the critical intensification factor (I_C) and the inverse value of electrical breakdown strength (E_B) for $BaTiO_3$ fiber filled composites; the solid line is the theoretical relation according to the equation in the figure.

breakdown threshold. That volume fraction might be too small to initiate global breakdown propagation through the bulk polymer considering the short term breakdown mechanisms such as electronic, thermal and electromechanical breakdown. Because only the field amplitude distribution and the threshold field strength are considered, the correlation between the field intensification factor and composite breakdown strength will be valid for any short term thermal or electronic breakdown mechanism, under the assumption that the breakdown mechanism is the same for the neat polymer and the composites. For long term breakdown behavior which might be related to partial discharge, treeing or electrochemical mechanisms, a much smaller probability value is expected because initiation depends on the most stressed region in the polymer.

The relation between I_C and E_B is plotted in Fig. 9b for $BaTiO_3$ fiber filled composites. The I_C for the neat polymer is unity since no field enhancement effect is present. The solid line shows the proposed relation in Eq. (5). All the results show good agreement with the proposed relation.

Although the chosen probability of 30% is an empirical to fit the data in this work, it is possible that this value is universal, considering an assumption that the highly stressed polymer region needs to reach percolation for the propagation of global breakdown. Whether this number would work in other systems needs further examination. The approach presented here addresses the change in breakdown strength with respect to the filler volume fraction and AR. Only a geometric factor of the inhomogeneous structure was considered in the study. Other influential factors, such as chemical species, thermal–mechanical behavior of composites and interfacial interaction between the polymer and fillers, are not evaluated. The role of interfacial regions might not stand out in this case, however, due to the sub-micron size of the fillers. Assuming a 10 nm interfacial layer thickness [31], the calculated interfacial volume fraction is about 5% for high AR $BaTiO_3$ fibers. For other systems in which other influential factors stand out, the proposed model might not be applicable.

3.2.3. Comparison with data in the literature

The proposed model in this work is also compared with the experimental data of $BaTiO_3$ particle filled composites in the literature [10] and the results are shown in Fig. 10. The characteristic probability of 30% was still used to obtain the estimated breakdown strength. The estimation matches the breakdown results well. The highest filler volume fraction that can be obtained in the FEA is 0.3, due to the Random Sequential Addition (RSA) method of the composite structure generation. A better algorithm is needed to predict the breakdown strength at a higher filler volume fraction.

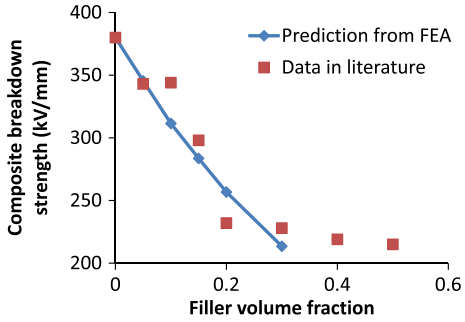

Fig. 10. Prediction of breakdown strength reported in the literature of $BaTiO_3$ particle filled composites [10] using the critical intensification factor model proposed in this work.

4. Summary

By FEA, several microstructure parameters of the composites filled with high AR fillers were studied for their impact on the composite permittivity, field distribution and breakdown strength. The geometric microstructure of composites was studied without introducing other influential factors such as the interfacial region between the filler and polymer matrix, and the defects introduced in the composite preparation process.

Several potential influential parameters of composite permittivity were analyzed individually and differentiated by the results. Their influence on the composite permittivity was compared to the rule of mixtures prediction and the experimental data. The difference in filler shape, the filler curvature and the low permittivity grain boundary in the high permittivity fillers have no influence on the composite permittivity. The distribution of fiber AR increases the composite permittivity, which did not lead to the smaller permittivity value observed in the experiment. Filler alignment in the compression molding process was determined to be responsible for the observed smaller composite permittivity compared to the rule of mixtures prediction.

The stress concentration in the polymer matrix caused by the high permittivity fillers was analyzed by FEA and a correlation between the field distribution statistics in the FEA and the experimental data of composite breakdown strength was established. It was speculated that the percolation of polymer regions sustaining higher electrical stress than the threshold value leads to the propagation of electrical breakdown. The proposed model was

used to successfully estimate the experimental data in the literature.

Acknowledgements

This work was supported by ABB and the Nanoscale Science and Engineering Center for Directed Assembly of Nanostructures at Rensselaer Polytechnic Institute under NSF Contract # DMR 0642573. One of us (H. Hillborg) also acknowledges support from the Swedish Research Council (IFA 2007-5095).

References

[1] Sihvola A. Mixing rules with complex dielectric coefficients. Subsurf Sens Technol Appl 2000;1:393–415.
[2] Ramaseshan R, Sundarrajan S, Jose R, Ramakrishna S. Nanostructured ceramics by electrospinning. J Appl Phys 2007;102:111101.
[3] Li D, McCann JT, Xia Y, Marquez M. Electrospinning: a simple and versatile technique for producing ceramic nanofibers and nanotubes. J Am Ceram Soc 2006;89:1861–9.
[4] Badrossamay MR, McIlwee HA, Goss JA, Parker KK. Nanofiber assembly by rotary jet-spinning. Nano Lett 2010;10:2257–61.
[5] Ju Z, Xu L, Pang Q, Xing Z, Ma X, Qian Y. The synthesis of nanostructured SiC from waste plastics and silicon powder. Nanotechnology 2009;20:355604.
[6] Liu D, Yan Y, Zhou H. Synthesis of micron-scale platelet $BaTiO_3$. J Am Ceram Soc 2007;90:1323–6.
[7] Myroshnychenko V, Brosseau C. Finite-element method for calculation of the effective permittivity of random inhomogeneous media. Phys Rev E 2005;71:016701.
[8] Krakovský I, Myroshnychenko V. Modeling dielectric properties of composites by finite-element method. J Appl Phys 2002;92:6743.
[9] Myroshnychenko V, Brosseau C. Finite-element modeling method for the prediction of the complex effective permittivity of two-phase random statistically isotropic heterostructures. J Appl Phys 2005;97:044101.
[10] Kim P, Doss NM, Tillotson JP, Hotchkiss PJ, Pan M-J, Marder SR, et al. High energy density nanocomposites based on surface-modified $BaTiO_3$ and a ferroelectric polymer. ACS Nano 2009;3:2581–92.
[11] Calame JP. Finite difference simulations of permittivity and electric field statistics in ceramic–polymer composites for capacitor applications. J Appl Phys 2006;99:084101.
[12] An L, Boggs SA, Calame JP. Energy storage in polymer films with high dielectric constant fillers. IEEE Electr Insul Mag 2008;24:5–10.
[13] Cheng Y, Chen X, Wu K, Wu S, Chen Y, Meng Y. Modeling and simulation for effective permittivity of two-phase disordered composites. J Appl Phys 2008;103:034111.
[14] Nilsson F, Gedde UW, Hedenqvist MS. Modelling the relative permittivity of anisotropic insulating composites. Compos Sci Technol 2011;71:216–21.
[15] Brosseau C, Beroual A, Boudida A. How do shape anisotropy and spatial orientation of the constituents affect the permittivity of dielectric heterostructures? J Appl Phys 2000;88:7278.
[16] Wang Z, Nelson JK, Miao J, Linhardt RJ, Schadler LS, Hillborg H, et al. Effect of high aspect ratio filler on dielectric properties of polymer composites: a study on barium titanate fibers and graphene platelets. IEEE Trans Dielectr Electr Insul 2012;19:960–7.
[17] Sihvola AH, Alanen E. Studies of mixing formulae in the complex plane. IEEE Trans Geosci Remote Sens 1991;29:679–87.
[18] Curecheriu L, Buscaglia MT, Buscaglia V, Zhao Z, Mitoseriu L. Grain size effect on the nonlinear dielectric properties of barium titanate ceramics. Appl Phys Lett 2010;97:242909.
[19] Wada S, Yasuno H, Hoshina T, Nam S-M, Kakemoto H, Tsurumi T. Preparation of nm-sized barium titanate fine particles and their powder dielectric properties. Jpn J Appl Phys 2003;42:6188–95.
[20] Ohara Y, Koumoto K, Yanagida H. Effect of crystal-axis orientation on dielectric properties of ceramics prepared from fibrous barium titanate. J Am Ceram Soc 1994;77:2327–31.
[21] Gao L, Zhai J, Song S, Yao X. Crystal orientation dependence of the out-of-plane dielectric properties for barium stannate titanate thin films. Mater Chem Phys 2010;124:192–5.
[22] Fang T-T, Hsieh H-L, Shiau F-S. Effects of pore morphology and grain size on the dielectric properties and tetragonal-cubic phase transition of high-purity barium titanate. J Am Ceram Soc 1993;76:1205–11.
[23] Takeuchi T, Tabuchi M, Ado K, Honjo K, Nakamura O, Kageyama H, et al. Grain size dependence of dielectric properties of ultrafine $BaTiO_3$ prepared by a sol–crystal method. J Mater Sci 1997;32:4053–60.
[24] Li X, Shih W-H. Size effects in barium titanate particles and clusters. J Am Ceram Soc 1997;80:2844–52.
[25] Hoshina T, Wada S, Kuroiwa Y, Tsurumi T. Composite structure and size effect of barium titanate nanoparticles. Appl Phys Lett 2008;93:192914.
[26] Uchino K, Sadanaga E, Hirose T. Dependence of the crystal structure on particle size in barium titanate. J Am Ceram Soc 1989;72:1555–8.
[27] Tsurumi T, Hoshina T, Takeda H, Mizuno Y, Chazono H. Size effect of barium titanate and computer-aided design of multilayered ceramic capacitors. IEEE Trans Ultrason Ferroelectr Freq Control 2009;56:1513–22.
[28] Takeuchi T, Ado K, Asai T, Kageyama H, Saito Y, Masquelier C, et al. Thickness of cubic surface phase on barium titanate single-crystalline grains. J Am Ceram Soc 1994;77:1665–8.
[29] Begg BD, Vance ER, Nowotny J. Effect of particle size on the room-temperature crystal structure of barium titanate. J Am Ceram Soc 1994;77:3186–92.
[30] Tsurumi T, Sekine T, Kakemoto H, Hoshina T, Nam S-M, Yasuno H, et al. Evaluation and statistical analysis of dielectric permittivity of $BaTiO_3$ powders. J Am Ceram Soc 2006;89:1337–41.
[31] Lewis TJ. Interfaces: nanometric dielectrics. J Phys D: Appl Phys 2005;38:202–12.